

# The shape and simplicity biases of adversarially robust ImageNet-trained CNNs

Peijie Chen · Chirag Agarwal · Anh Nguyen

the date of receipt and acceptance should be inserted later

**Abstract** Adversarial training has been the topic of dozens of studies and a leading method for defending against adversarial attacks. Yet, it remains largely unknown (a) how adversarially-robust ImageNet classifiers (R classifiers) generalize to out-of-distribution examples; and (b) how their generalization capability relates to their hidden representations. In this paper, we perform a thorough, systematic study to answer these two questions across AlexNet, GoogLeNet, and ResNet-50 architectures. We found that while standard ImageNet classifiers have a strong texture bias, their R counterparts rely heavily on shapes. Remarkably, adversarial training induces three simplicity biases into hidden neurons in the process of “robustifying” the network. That is, each convolutional neuron in R networks often changes to detecting (1) pixel-wise smoother patterns i.e. a mechanism that blocks high-frequency noise from passing through the network; (2) more lower-level features i.e. textures and colors (instead of objects); and (3) fewer types of inputs. Our findings reveal the interesting mechanisms that made networks more adversarially robust and also explain some recent findings e.g. why R networks benefit from much larger capacity (Xie and Yuille, 2020) and can act as a strong image prior in image synthesis (Santurkar et al., 2019).

**Keywords** Deep Learning · Computer Vision · Robustness · Adversarial Training · Interpretability · Texture · Shape

All authors contributed equally.

Peijie Chen · Chirag Agarwal · Anh Nguyen  
Auburn University, Department of Computer Science and  
Software Engineering, Auburn, AL 36849, USA  
E-mail: anh.ng8@gmail.com

## 1 Introduction

Human vision has been long known to be shape-biased i.e. recognizing an object by relying on its outline or silhouette as opposed to texture cues (Geirhos et al., 2019). This shape bias was hypothesized to contribute to the superior performance of humans on out-of-distribution (OOD) data (Geirhos et al., 2018), compared to state-of-the-art convolutional neural networks (CNNs), which rely heavily on textures (Geirhos et al., 2019).

A current, large gap between modern machine and human intelligence is in flexible, systematic, OOD generalization (Goyal and Bengio, 2020). For example, despite excellent test-set performance, CNNs often misclassify out-of-samples (Nguyen et al., 2015) including “*adversarial examples*”, i.e. modified inputs that are imperceptibly different from the real data but change predicted labels entirely (Szegedy et al., 2014). A leading method to combat this issue is adversarial training—teaching a classifier to correctly label adversarial examples instead of real examples (Madry et al., 2018). In addition, test-set accuracy can also be improved, for some architectures, when real images are properly incorporated into adversarial training (Xie et al., 2020).

We aim to study the relation between the shape bias of adversarially-robust CNNs and their generalizability induced by adversarial training by asking:

**Q1:** *On ImageNet, do adversarially-robust networks (hereafter, R networks) prefer shapes over textures?*

It remains unknown whether a *shape* bias exists in networks trained on the large-scale ImageNet (Rusakovsky et al., 2015), which often induces a large *texture* bias into networks (Geirhos et al., 2019) e.g. to separate  $\sim 150$  four-legged species in ImageNet. This question is also important because the recent findings suggest that ImageNet-trained R networks act as a strong

image *texture* prior i.e. they can be successfully used for many pixel-wise image optimization tasks (Santurkar et al., 2019). The above discussion leads to a follow-up question:

**Q2:** *If an R network has a stronger preference for shapes than standard ImageNet-trained CNNs (hereafter, S networks), will it perform better on OOD images?*

This important link was not yet established. That is, Geirhos et al. (2019) found that CNNs trained to be more *shape*-biased (but *not* via adversarial training) can generalize better to many unseen ImageNet-C (Hendrycks and Dietterich, 2019) image corruptions than S networks, which have a much weaker shape bias (Brendel and Bethge, 2019). In contrast, R networks, which were trained solely on adversarial examples, often *underperform* S networks on real test sets (Tsipras et al., 2019) perhaps due to an inherent trade-off (Madry et al., 2018), a mismatch between real vs. adversarial distributions (Xie et al., 2020), or a limitation in architectures—AdvProp did not improve the test-set performance of ResNets (Xie et al., 2020).

Most previous work aimed at understanding the behaviors of R classifiers as a function but little is known about the internal characteristics of R networks and, furthermore, their connections to the shape bias and performance on OOD data. Here, we ask:

**Q3:** *How did adversarial training change the hidden neural representations to make CNNs more shape-biased and adversarially-robust?*

In this paper, we harness three common datasets in ML interpretability and neuroscience—cue-conflict (Geirhos et al., 2019), NetDissect (Bau et al., 2017), and ImageNet-C—to answer the three questions above via a systematic study across three different convolutional architectures—AlexNet (Krizhevsky et al., 2012), GoogLeNet (Szegedy et al., 2015), and ResNet-50 (He et al., 2016)—trained to perform image classification on the large-scale ImageNet dataset (Russakovsky et al., 2015). Our main findings include:

1. R classifiers trained on ImageNet prefer shapes over textures  $\sim 67\%$  of the time—a stark contrast to S classifiers, which prefer shapes at  $\sim 25\%$  (Sec. 3.1).
2. Consistent with the strong shape bias, R classifiers interestingly outperform S counterparts on textureless, distorted images (stylized and silhouetted images) (Sec. 3.2.2).
3. Adversarial training makes CNNs more robust by (a) blocking pixel-wise input noise via smooth filters (Sec. 3.3.1); (b) reducing the set of high-activating inputs to simple patterns (Sec. 3.3.2).
4. Units that detect texture patterns (according to NetDissect) are not only useful to texture-based image

classification but can be also highly useful to *shape*-based classification (Sec. 3.4).

5. By aligning NetDissect and cue-conflict frameworks, we found that hidden neurons in R networks are surprisingly neither strongly shape-biased nor texture-biased, but instead generalists that detect low-level features (Sec. 3.4).

## 2 Networks and Datasets

**Networks** To understand the effects of adversarial training across a wide range of architectures, we compare each pair of S and R models while keeping their network architectures constant. That is, we conduct all experiments on two groups of classifiers: (a) standard AlexNet, GoogLeNet, & ResNet-50 (hereafter, ResNet) models pre-trained on the 1000-class 2012 ImageNet dataset; and (b) three adversarially-robust counterparts i.e. AlexNet-R, GoogLeNet-R, & ResNet-R which were trained via adversarial training (see below).

**Training** A standard classifier with parameters  $\theta$  was trained to minimize the cross-entropy loss  $L$  over pairs of (training example  $x$ , ground-truth label  $y$ ) drawn from the ImageNet training set  $\mathcal{D}$ :

$$\arg \min_{\theta} \mathbb{E}_{(x,y) \sim \mathcal{D}} [L(\theta, x, y)] \quad (1)$$

On the other hand, we trained each R classifier via Madry et al. (2018) adversarial training framework where each real example  $x$  is changed by a perturbation  $\Delta$ :

$$\arg \min_{\theta} \mathbb{E}_{(x,y) \sim \mathcal{D}} \left[ \max_{\Delta \in \mathcal{P}} L(\theta, x + \Delta, y) \right] \quad (2)$$

and  $\mathcal{P}$  is the perturbation range allowed within an  $L_2$  norm.

**Hyperparameters** The S models were downloaded from PyTorch model zoo (PyTorch, 2019). We adversarially trained all R models using the **robustness** library (Engstrom et al., 2019), using *the same* hyperparameters in (Engstrom et al., 2020; Santurkar et al., 2019; Bansal et al., 2020) because these previous works have shown that adversarial training significantly changed the inner-workings of ImageNet CNNs—i.e. becoming a strong image prior with perceptually-aligned deep features. That is, adversarial examples were generated using Projected Gradient Descent (PGD) (Madry et al., 2018) with an  $L_2$  norm constraint  $\epsilon$  of 3, a step size of 0.5, and 7 PGD-attack steps. R models were trained using an SGD optimizer for 90 epochs with a momentum of 0.9, an initial learning rate of 0.1 (which is reduced

Table 1: Top-1 accuracy (%) on 50K-image ImageNet validation-set and PGD adversarial examples.

	AlexNet	AlexNet-R	GoogLeNet	GoogLeNet-R	ResNet	ResNet-R
ImageNet	<b>56.52</b>	39.83	<b>69.78</b>	43.57	<b>76.13</b>	57.90
Adversarial	0.18	<b>22.27</b>	0.08	<b>31.23</b>	0.35	<b>36.11</b>

Table 2: While standard classifiers rely heavily on textures, R classifiers rely heavily on shapes. The top-1 accuracy scores (%) are computed on the cue-conflict dataset by Geirhos et al. (2019).

	AlexNet	AlexNet-R	GoogLeNet	GoogLeNet-R	ResNet	ResNet-R
Texture	<b>73.61</b>	34.67	<b>74.91</b>	34.43	<b>77.79</b>	29.63
Shape	26.39	<b>65.32</b>	25.08	<b>65.56</b>	22.20	<b>70.36</b>

10 times every 30 epochs), a weight decay of  $10^{-4}$ , and a batch size of 256 on 4 Tesla-V100 GPU’s.

Compared to the standard counterparts, R models have substantially higher adversarial accuracy but lower ImageNet validation-set accuracy (Table 1). To compute adversarial accuracy, we perturbed validation-set images with the same PGD attack settings as used in training.

#### Correctly-labeled image subsets: ImageNet-CL

Following Bansal et al. (2020), to compare the behaviors of two networks of identical architectures on the same inputs, we tested them on the largest ImageNet validation subset (hereafter, ImageNet-CL) where both models have 100% accuracy. The sizes of the three subsets for three architectures—AlexNet, GoogLeNet, and ResNet—are respectively: 17,693, 20,238, and 27,343. On modified ImageNet images (e.g. ImageNet-C), we only tested each pair of networks on the modified images whose original versions exist in ImageNet-CL. That is, we wish to gain deeper insights into how networks behave on correctly-classified images, and then how their behaviors change when some input feature (e.g. textures or shapes) is modified.

### 3 Experiment and Results

#### 3.1 Do ImageNet adversarially-robust networks prefer shapes or textures?

It is important to know which type of feature a classifier uses when making decisions. While standard ImageNet networks often carry a strong texture bias (Geirhos et al., 2019), it is unknown whether their adversarially-robust counterparts would be heavily texture- or shape-biased. Here, we test this hypothesis by comparing S and R models on the well-known cue-conflict dataset (Geirhos et al., 2019). That is, we feed “stylized” images provided by Geirhos et al. (2019) that contain con-

tradicting texture and shape cues (e.g. elephant skin on a cat silhouette) and count the times a model uses textures or shapes (i.e. outputting elephant or cat) when it makes a correct prediction.

**Experiment** Our procedure follows Geirhos et al. (2019). First, we excluded 80 images that do not have conflicting cues (e.g. cat textures on cat shapes) from their 1,280-image dataset. Each texture or shape cue belongs to one of 16 MS COCO (Caesar et al., 2018) coarse labels (e.g. cat or elephant). Second, we ran the networks on these images and converted their 1000-class probability vector outputs into 16-class probability vectors by taking the average over the probabilities of the fine-grained classes that are under the same COCO label. Third, we took only the images that each network correctly labels (i.e. into the texture or shape class), which ranges from 669 to 877 images (out of 1,200) for 6 networks and computed the texture and shape accuracies over 16 classes.

**Results** On average, over three architectures, R classifiers rely on shapes  $\geq 67.08\%$  of the time i.e.  $\sim 2.7\times$  higher than 24.56% of the S models (Table 2). In other words, by replacing the real examples with adversarial examples, adversarial training causes the heavy texture bias of ImageNet classifiers (Geirhos et al., 2019; Brendel and Bethge, 2019) to drop substantially ( $\sim 2.7\times$ ).

#### 3.2 Do robust networks generalize to unseen types of distorted images?

We have found that changing from standard training to adversarial training changes ImageNet CNNs entirely from texture-biased into shape-biased (Sec. 3.1). Furthermore, Geirhos et al. (2019) found that some training regimes that encourage classifiers to focus more on *shape* can improve their performance on unseen image distortions. Therefore, it is interesting to test whether

Table 3: Adversarially-robust (R) models outperform vanilla (S) models when both are under PGD-adversarial attacks (b). While R models do not generalize well to common distortions (c), yet, they interestingly outperform S models on texture-less images (e–f). Here, we report top-1 accuracy scores (%) on the transformed images whose original real versions were correctly-labeled (a) by both S and R models. “ImageNet-C” column (c) shows the mean accuracy scores over all 15 distortion types (see breakdown accuracy on each distortion type in Table A1). “Scrambled” column (d) shows the mean accuracy scores over three patch-scrambling types (details in Fig. 3).

Network	(a) Real ImageNet	(b) Adversarial	Shape-less				
			(c) ImageNet-C	(d) Scrambled	(e) Stylized	(f) B&W	(g) Silhouette
AlexNet	100	0.18	35.06	<b>34.59</b>	6.31	20.08	7.72
AlexNet-R	100	<b>22.27</b>	<b>44.94</b>	16.92	<b>9.11</b>	<b>35.25</b>	<b>9.30</b>
GoogLeNet	100	0.08	<b>58.27</b>	<b>49.74</b>	13.74	43.48	10.17
GoogLeNet-R	100	<b>31.23</b>	38.76	31.15	12.54	<b>44.55</b>	<b>24.12</b>
ResNet	100	0.35	<b>56.92</b>	<b>58.04</b>	10.68	16.96	3.95
ResNet-R	100	<b>36.11</b>	48.80	34.46	<b>15.62</b>	<b>53.89</b>	<b>22.30</b>

(a) Real (b) Adversarial (c) ImageNet-C (d) Scrambled (e) Stylized (f) B&W (g) Silhouette



Fig. 1: Example distorted images (b–g). We show an example Gaussian-noise-added image (c) out of all 15 ImageNet-C types. See Fig. A5 for more examples.

R models—a type of *shape*-biased classifiers— would generalize well to any OOD image types.

**ImageNet-C** We compare S and R networks on the ImageNet-C, which was designed to test model robustness on 15 common types of image corruptions (Fig. 1c), where several shape-biased classifiers trained on stylized images were known to outperform S classifiers (Geirhos et al., 2019). Here, we tested each pair of S and R models on the ImageNet-C distorted images whose original versions were correctly labeled by both (i.e. in ImageNet-CL sets; Sec. 2).

**Results** Interestingly, R models show no generalization boost on ImageNet-C, i.e. they performed on-par or worse than the S counterparts (Table 3c). However, because ImageNet-C contains a variety of image distortions that change both textures and shapes, it is not possible to attribute an improved ImageNet-C performance to the shape bias.

To further understand the generalizability of R models, we tested them on two *controlled* image types where either shape or texture cues are removed from the original, correctly-labeled ImageNet images (Fig. 1d–g). Note that when both shape and texture cues are present e.g. in cue-conflict images, R classifiers consistently prefer shape over texture i.e. a shape *bias*. However, this bias may not necessarily carry over to the images where only either texture or shape cues are present.

### 3.2.1 Performance on shape-less images

We created shape-less images by dividing each ImageNet-CL image into a grid of  $p \times p$  even patches where  $p \in \{2, 4, 8\}$  and re-combining them randomly into a new “scrambled” version (Fig. 1d). On average, over three grid types, we observed a larger accuracy drop in R models compared to S models, ranging from  $1.6\times$  to  $2.04\times$  lower accuracy (Table 3d). That is, **R model performance drops substantially more than S models when object shapes are removed**—another evidence for their reliance on shapes. See Fig. 2 for the predictions of ResNet and ResNet-R on patch-scrambled images.

### 3.2.2 Performance on texture-less images

Following Geirhos et al. (2019), we tested R models on three types of texture-less images where the texture is increasingly removed: (1) stylized ImageNet images where textures are randomly modified; (2) binary, black-and-white, i.e. B&W, images (Fig. 1f); and (3) silhouette images where the texture information is completely removed (Fig. 1e, g).

**Stylized ImageNet** To construct a set of stylized ImageNet images (see Fig. 1e), we took all ImageNet-CL images (Sec. 2) and changed their textures via a styliza-

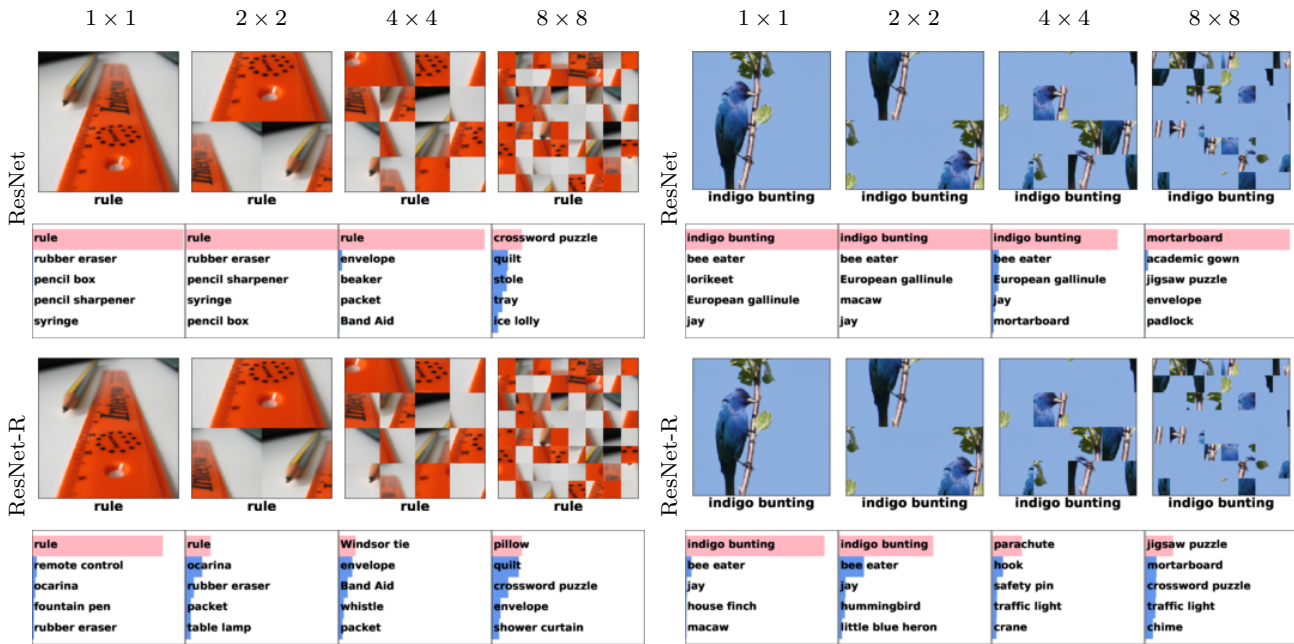


Fig. 2: Qualitative examples showing the strong *texture* bias of standard CNNs (here, ResNet) and the strong *shape* bias of adversarially-robust models (here, ResNet-R) as described in Sec. 3.2.1. When patches are scrambled, ResNet-R confidence drops substantially and its **top-1 predicted** labels often change away from the original, correctly-predicted label, here, rule (left) and indigo bunting (right).

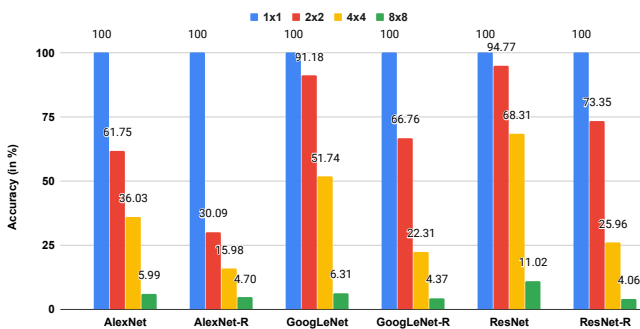


Fig. 3: Standard CNNs substantially outperform R models on scrambled versions of the ImageNet-CL images due to their capability of recognizing images using textures. Here, we report top-1 accuracy (%) on the scrambled images whose original versions (ImageNet-CL) were correctly-labeled by both standard and R classifiers (hence, the 100% for  $1 \times 1$  blue bars).

tion procedure in Geirhos et al. (2019), which harnesses the style transfer technique (Gatys et al., 2016) to apply a random style to each ImageNet “content” image.

**B&W images** For all ImageNet-CL images, we used the same process described in Geirhos et al. (2019) to generate silhouettes, but we did not manually select or modify the images. We used ImageMagick (2020) to

binarize ImageNet images into B&W images via the following steps:

```
convert image.jpeg image.bmp
potrace -svg image.bmp -o image.svg
rsvg-convert image.svg > image.jpeg
```

**Silhouette** For all ImageNet-CL images, we obtained their segmentation maps via a PyTorch DeepLab-v2 model (Chen et al., 2017) pre-trained on MS COCO-Stuff. We used the ImageNet-CL images that belong to a set of 16 COCO coarse classes in Geirhos et al. (2019) (e.g. bird, bicycle, airplane, etc.). When evaluating classifiers, an image is considered correctly labeled if its ImageNet predicted label is a subclass of the correct class among the 16 COCO classes (Fig. 1g; mapping sandpiper  $\rightarrow$  bird).

**Results** Consistently, **on all three texture-less image sets, R models outperformed their S counterparts** (Table 3e–g)—a remarkable generalization capability, especially on B&W and silhouette images where little to no texture information is available.

### 3.3 What internal mechanisms make adversarially trained CNNs more robust than standard CNNs?

We have shown that after adversarial training, R models are more robust than S models on new adversar-

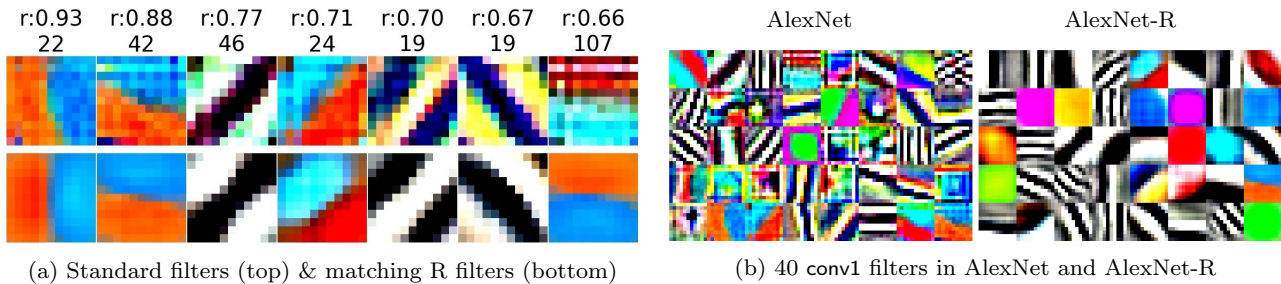


Fig. 4: **Left:** For each AlexNet conv1 filter (top row), we show the highest-correlated filter in AlexNet-R (bottom row), their Spearman rank correlation (e.g.  $r: 0.93$ ) and the Total Variation (TV) difference (e.g. 22) between the top kernel and the bottom. Here, the TV differences are all positive i.e. AlexNet filters have higher TV. See Fig.A2 for full plot. **Right:** conv1 filters of AlexNet-R are smoother and less diverse than the counterparts. See Figs. A1 for GoogLeNet & ResNet.

Table 4: Mean total variation (TV) of the conv layers of 6 models.

	AlexNet	AlexNet-R	GoogLeNet	GoogLeNet-R	ResNet	ResNet-R
Mean TV	110.20	<b>63.59</b>	36.53	<b>22.79</b>	18.35	19.96

ial examples generated for these pre-trained models via PGD attacks (Table 3b). Furthermore, on non-adversarial, high-frequency images, R models may also outperform S models (Table A1a; AlexNet-R) (Yin et al., 2019; Gilmer et al., 2019).

We aim to understand the internal mechanisms that make R CNNs more robust to high-frequency noise by analyzing the networks at the weight (Sec. 3.3.1) and neuron (Sec. 3.3.2) levels.

### 3.3.1 Weight level: Smooth filters to block pixel-wise noise

**Smother filters** To explain this phenomenon, we visualized the weights of all 64 conv1 filters ( $11 \times 11 \times 3$ ), in both AlexNet and AlexNet-R, as RGB images. We compare each AlexNet conv1 filter with its nearest conv1 filter (via Spearman rank correlation) in AlexNet-R. Remarkably, R filters appear qualitatively much smoother than their counterparts (Fig. 4a). The R filter bank is also less diverse, e.g. R edge detectors are often black-and-white in contrast to the colorful AlexNet edges (Fig. 4b). A similar contrast was also seen for the GoogLeNet and ResNet models (Fig. A1).

We also quantify the smoothness, in total variation (TV) (Rudin et al., 1992), of the filters of all 6 models (Table 4) and found that, on average, the filters in R networks are much smoother. For example, the mean TV of GoogLeNet-R is about 1.5 times smaller than that of GoogLeNet. In almost all layers, R filters are smoother than S filters (Fig. A9).

**Blocking pixel-wise noise** We hypothesize that the smoothness of filters makes R classifiers more robust against noisy images. To test this hypothesis, we computed the total variation of the channels across 5 conv layers when feeding ImageNet-CL images and their noisy versions (Fig. 1c; ImageNet-C Level 1 additive noise  $\sim N(0, 0.08)$ ) to S and R models.

At conv1, the smoothness of R activation maps remains almost unchanged before and after noise addition (Fig. 5a; yellow circles are on the diagonal line). In contrast, the conv1 filters in standard AlexNet allow Gaussian noise to pass through, yielding larger-TV channels (Fig. 5a; blue circles are mostly above the diagonal). That is, the smooth filters in **R models indeed can filter out pixel-wise Gaussian noise despite that R models were not explicitly trained on this image type!**

In higher layers, it is intuitive that the pixel-wise noise added to the input image might not necessarily cause activation maps, in both S and R networks, to be noisy because higher-layered units detect more abstract concepts. However, interestingly, we still found that R channels to have consistently less mean TV (Fig. 5b–c). Our result suggests that most of the de-noising effects take place at lower layers (which contain more generic features) instead of higher layers (which contain more task-specific features).

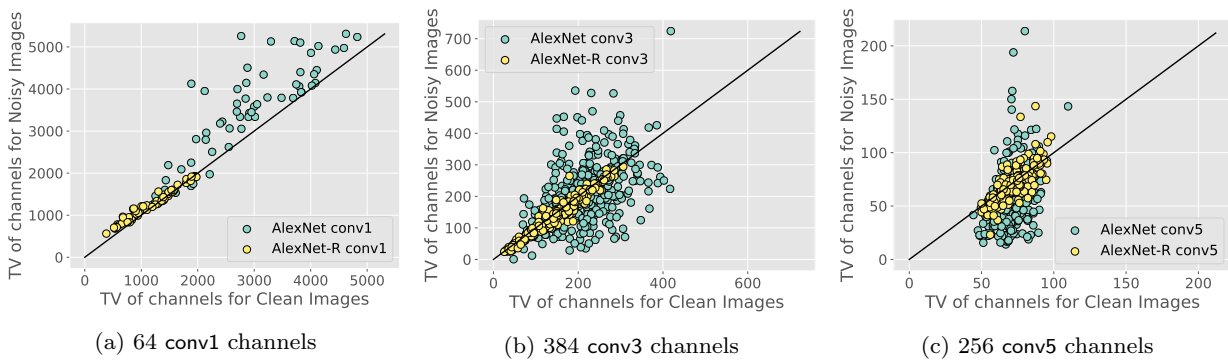


Fig. 5: In each subpanel, one point shows the mean Total Variation (TV) of one channel when running clean ImageNet-CL images and their noisy versions through AlexNet (●) or AlexNet-R (●). R channels have similar TV before and after adding noise, suggesting that conv1 kernels filter out the added noise. In higher layers (conv3 and conv5), R channels are consistently more invariant to the input noise than S channels (● dots are clustered around the diagonal line while ● dots have higher variance). See Fig. A4 for the same scatter plot (a) for all five layers.

### 3.3.2 Neuron level: Robust neurons prefer lower-level and fewer inputs

Here, via NetDissect framework, we wish to characterize how adversarial training changed the hidden neurons in R networks to make R classifiers more adversarially robust.

**Network Dissection** (hereafter, NetDissect) is a common framework for quantifying the functions of a neuron by computing the Intersection over Union (IoU) between each activation map (i.e. channels) and the human-annotated segmentation maps for the same input images. That is, each channel is given an IoU score per human-defined concept (e.g. *dog* or *zigzagged*) indicating its accuracy in detecting images of that concept. A channel is tested for its accuracy on all  $\sim 1,400$  concepts, which span across six coarse categories: **object**, **part**, **scene**, **texture**, **color**, and **material** (Bau et al., 2017) (c.f. Fig. A11 for example NetDissect images in *texture* and *color* concepts). Following Bau et al. (2017), we assign each channel  $C$  a main functional label i.e. the concept that  $C$  has the highest IoU with. In both S and R models, we ran NetDissect on all 1152, 5808, and 3904 channels from, respectively, 5, 12, and 5 main convolutional layers (post-ReLU) of the AlexNet, GoogLeNet, and ResNet-50 architectures (c.f. Sec. A for more details of layers used).

**Shift to detecting more low-level features i.e. colors and textures** We found a consistent trend—adversarial training resulted in substantially more filters that detect colors and textures (i.e. in R models) in exchange for fewer object and part detectors. For example, throughout the same GoogLeNet architecture, we observed a 102% and a 34% increase of color and texture detectors, respectively, in the R model, but a 20%

and a 26% fewer object and part detectors, compared to the S model (c.f. Fig. 6a). After adversarial training,  $\sim 11\%$ ,  $15\%$ , and  $10\%$  of all hidden neurons (in the tested layers) in AlexNet, GoogLeNet, and ResNet, respectively, shift their roles to detecting lower-level features (i.e. textures and colors) instead of higher-level features (see feature visualizations in Fig. 7).

Across three architectures, the increases in texture and color channels are often larger in higher layers. The largest functional shifts appearing in higher layers can be because the higher-layered units are more task-specific (Nguyen et al., 2016a; Yosinski et al., 2014).

**Consistent findings with ResNet CNNs trained on Stylized ImageNet** We also compare the shape-biased ResNet-R with ResNet-SIN, i.e. a ResNet-50 trained exclusively on stylized ImageNet images where textures are removed via stylization (Geirhos et al., 2019). ResNet-SIN also has a strong shape bias of 81.37%.<sup>1</sup> Interestingly, similar to ResNet-R, ResNet-SIN also has more low-level feature detectors (colors and textures) and fewer high-level feature detectors (objects and parts) than the vanilla ResNet (Fig. 8). In contrast, finetuning this ResNet-SIN on ImageNet remarkably changes the model to be *texture-biased* (at a 79.7% texture bias) and to contain fewer texture and more object and part units (Fig. 8; ResNet-SIN+IN vs. ResNet-SIN). That is, training or finetuning on ImageNet tend to cause CNNs to be more texture-biased and contain more high-level features (i.e. detecting objects and parts). In contrast, training on adversarial examples or texture-distorted images cause CNNs to focus more on shapes and learn more generic, low-level features.

<sup>1</sup> model\_A in <https://github.com/rgeirhos/texture-vs-shape/>. See Table 4 in Geirhos et al. (2019).

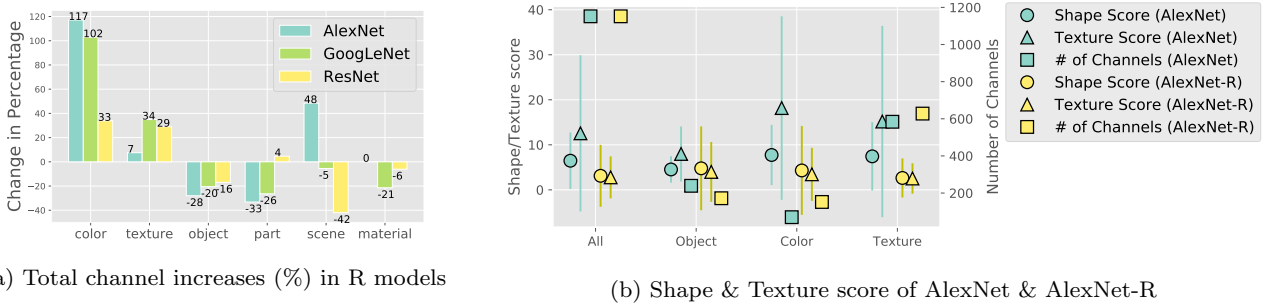


Fig. 6: **Left:** For all three architectures, the numbers of NetDissect *color* and *texture* detectors in R models increase, e.g. by 117% and 7%, respectively, for AlexNet, while the number of *object* units decreases by 28% (a). See Fig. A3 for layer-wise plots for detectors in other category. **Right:** The average Shape (●) and Texture (▲) scores over all channels in the entire network (“All”) or in a NetDissect category (“Object”, “Color”, and “Texture”). While AlexNet-R has more *color* and *texture* channels (■ above ■), these R channels are not heavily shape- or texture-biased. In contrast, the corresponding channels in AlexNet are heavily texture-biased (▲ is almost 2× of ●).

**Shift to detecting simpler objects** Analyzing the concepts in the *object* category where we observed largest changes in channel count, we found evidence that neurons change from detecting complex to simpler objects. That is, for each NetDissect concept, we computed the difference in the numbers of channels between the S and R model. In the same *object* category, AlexNet-R model has substantially fewer channels detecting complex concepts e.g.  $-30$  *dog*,  $-13$  *cat*, and  $-11$  *person* detectors (Fig. A10b; rightmost columns), compared to the standard network. In contrast, the R model has more channels detecting simpler concepts, e.g.  $+40$  *sky* and  $+12$  *ceiling* channels (Fig. A10b; leftmost columns). The top-49 images that highest-activated R units across five conv layers also show their strong preference for simpler backgrounds and objects (Fig. 7).

**Shift to detecting fewer unique concepts** The previous sections have revealed that neurons in R models often prefer images that are pixel-wise smoother (Sec. 3.3.1) and of lower-level features (Sec. 3.3.2), compared to S neurons. Another important property of the complexity of the function computed at each neuron is the diversity of types of inputs detected by the neuron (Nguyen et al., 2016b, 2019). Here, we compare the diversity score of NetDissect concepts detected by units in S and R networks. For each channel  $C$ , we calculated a diversity score, i.e. the number of unique concepts that  $C$  detects with an IoU score  $\geq 0.01$ .

Interestingly, on average, an R unit fires for 1.16 times fewer unique concepts than an S unit (22.43 vs. 26.07; c.f. Fig. A12a). Similar trends were observed in ResNet (Fig. A12b). Qualitatively comparing the highest-activation training-set images by the highest-IoU channels in both networks, for the same most-frequent concepts (e.g. *striped*), often confirms a striking differ-

ence: R units prefer a less diverse set of inputs (Fig. 7). As R hidden units fire for fewer concepts, i.e. significantly fewer inputs, the space for adversarial inputs to cause R models to misbehave is strictly smaller.

### 3.4 Which neurons are important for shape-based or texture-based image classification?

To understand how the found changes in R neurons (Sec. 3.3) relate to the shape bias of R CNNs (Sec. 3.1), here, we zero out every channel, one at a time, in S and R networks and measure the performance drop in recognizing shapes and textures from cue-conflict images. **Shape & Texture scores** For each channel, we computed a “Shape score”, i.e. the number of images originally correctly labeled into the *shape* class by the network but that, after the ablation, are labeled differently (examples in Fig 9a–b). Similarly, we computed a Texture score per channel. The Shape and Texture scores quantify the importance of a channel in image classification using shapes and textures, respectively.

First, we found that the **channels labeled texture by NetDissect are not only important to texture-based but also shape-based classification**. That is, on average, zero-ing out these channels caused non-zero Texture and Shape scores (Fig. 6b; Texture ● and ▲ are above 0). See Fig. 9 for an example of texture channels with high Shape and Texture scores. This result is aligned with the fact that R networks consistently have more *texture* units (Fig. 6a) but are shape-biased (Sec. 3.1).

Second, the *texture* units are, as expected, highly texture-biased in AlexNet (Fig. 6b Texture; ▲ is almost 2× of ●). However, surprisingly, those **texture units in AlexNet-R are neither strongly shape-biased**

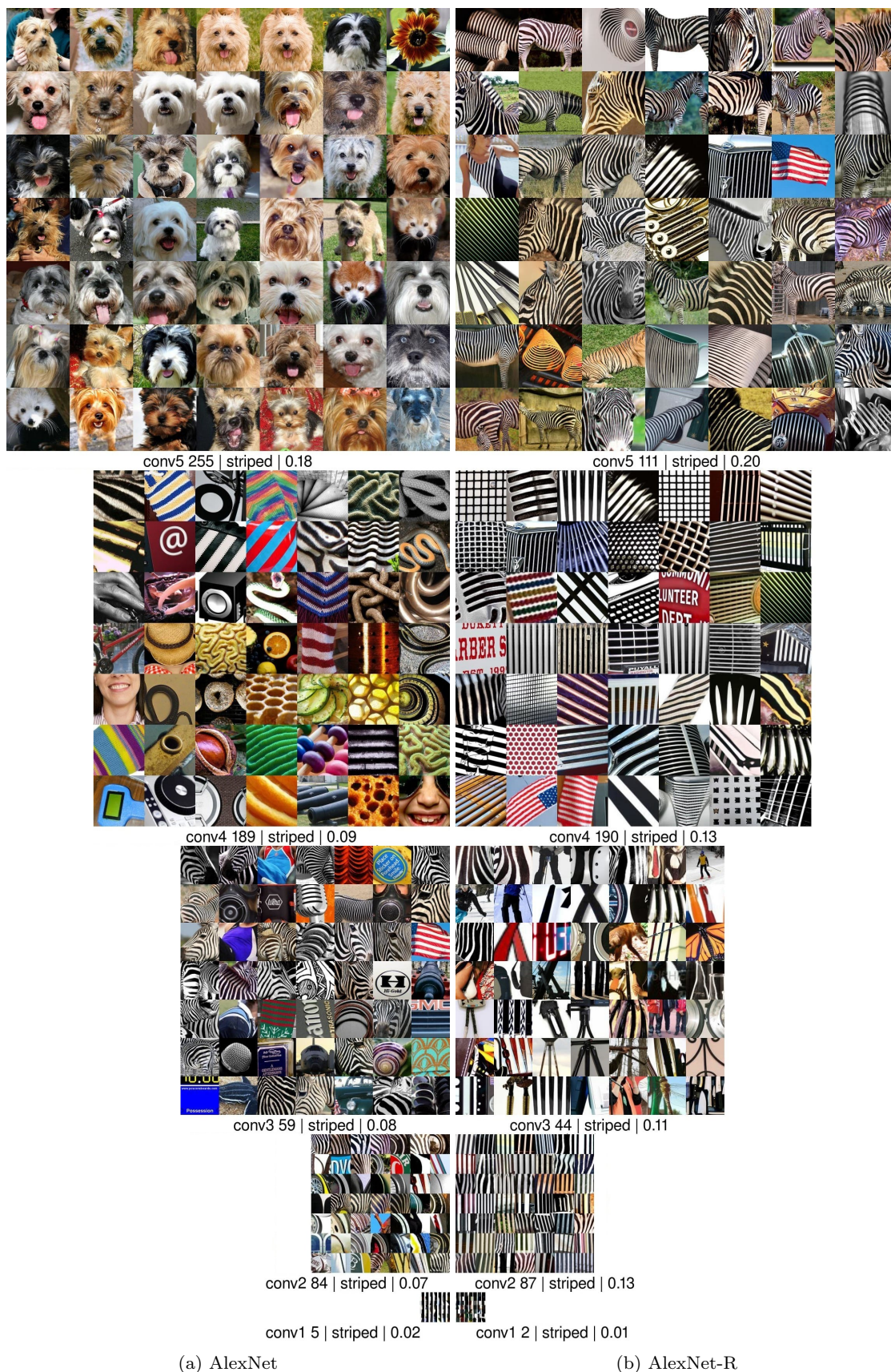


Fig. 7: Each  $7 \times 7$  grid shows the top-49 training-set images that highest activate the center unit in a channel. Each column shows five highest-IoU striped concept channels, each from one AlexNet's conv layer in their original resolutions. From top to bottom, AlexNet-R (b) consistently preferred striped patterns, i.e., edges (conv1), vertical bars (conv2), tools, to grids and zebra (conv5). In contrast, AlexNet striped images (a) are much more diverse, including curly patterns (conv4) and dog faces (conv5).

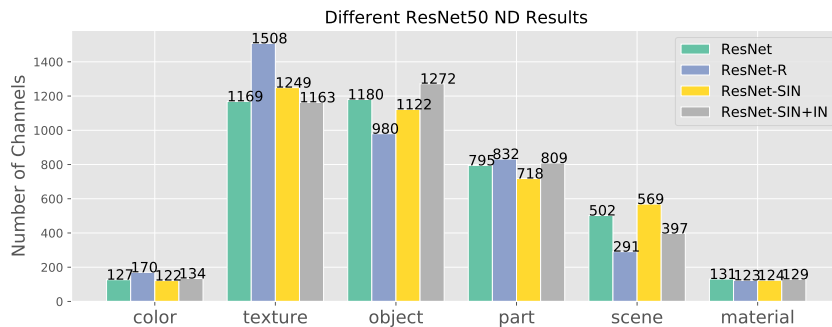


Fig. 8: Each column shows the number of channels (in a ResNet-50 model) categorized into one of NetDissect categories. For example, the standard ImageNet-trained ResNet has 127 color detectors (leftmost column). Here, we compare the neural functions among four different ResNet-50 models trained differently: (1) ResNet was trained on ImageNet; (2) ResNet-R was trained via PGD-adversarial training; (3) ResNet-SIN was trained on texture-removed ImageNet from (Geirhos et al., 2019); and (4) ResNet-SIN+IN was a ResNet-SIN that was then finetuned on ImageNet. Training on texture-removed ImageNet or adversarial examples consistently produces CNNs that are (a) heavily shape-biased; (b) contain more low-level, texture features; (c) fewer high-level, object detectors compared to training on ImageNet which produces texture-biased CNNs (ResNet and ResNet-SIN+IN).

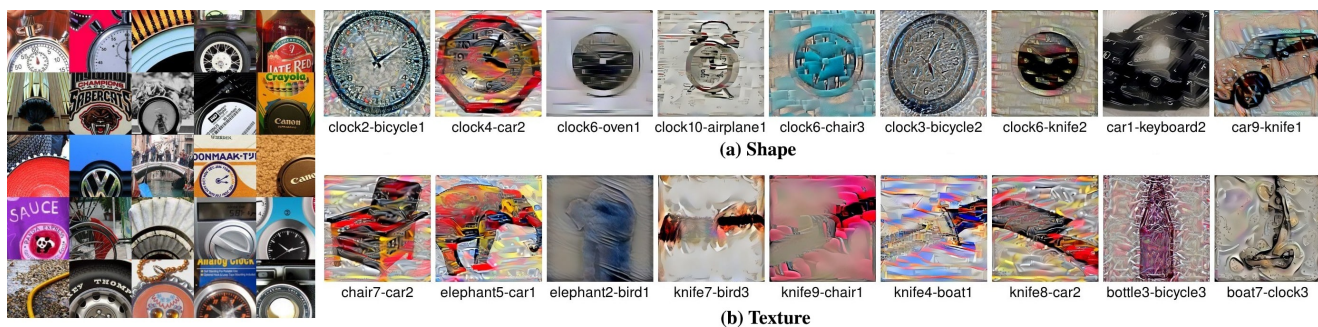


Fig. 9: **Left:** Top-25 highest-activation images of the AlexNet unit  $\text{conv4}_{19}$ , which has a NetDissect label of spiralled under texture category. The unit prefers circular patterns including car wheels and clock. **Right:** Example *cue-conflict* images originally labeled by AlexNet as shape (top) or texture (bottom) but that were given a different label after the unit  $\text{conv4}_{19}$  is ablated. For example, “clock2-bicycle1” is a cue-conflict image that has the shape of a clock and the texture of a bicycle. Qualitatively, the unit helps AlexNet detect clocks and cars using shapes (top) and reddish pink cars, birds, chairs, and bicycles using textures (bottom). The unit has Shape and Texture scores of 18 and 22, respectively. See Fig. A6 & Fig. A7 for more examples.

**nor texture-biased** (Fig. 6b; Texture  $\bullet \approx \blacktriangle$ ). That is, across all three groups of the object, color, and texture, **R neurons appear mostly to be generalist, low-level feature detectors**. This generalist property might be a reason for why R networks are more effective in transfer learning than S networks (Salman et al., 2020).

Finally, the contrast above between the texture bias of S and R channels (Fig. 6b) reminds researchers that the single semantic label assigned by NetDissect to each neuron is not describing a full picture of what the neuron does and how it helps in downstream tasks. To the best of our knowledge, this is the first work to align the NetDissect and cue-conflict frameworks to study

how individual neurons contribute to the generalizability and shape bias of the entire network.

## 4 Related Work

**Shape bias** On smaller-scaled datasets e.g. CIFAR-10, Zhang and Zhu (2019) also found that R networks rely heavily on shapes (instead of textures) to classify images. However, such shape bias may not necessarily generalize to high-dimensional, large-scale datasets such as ImageNet. Different from Zhang and Zhu (2019), here, we study networks trained on ImageNet and its variants (e.g. Stylized ImageNet). To the best of our

knowledge, we are the first to reveal (1) the shape bias of ImageNet-trained R networks; (2) the roles of neurons in R networks; and (3) their internal robustification mechanisms. We also found that our adversarially-trained CNNs and the CNNs trained on texture-removed images by Geirhos et al. (2019) both similar have a strong shape bias and contain simpler and more generic features than standard ImageNet-trained CNNs.

**Simplicity bias** Deep neural networks tend to prioritize learning simple patterns that are common across the training set (Arpit et al., 2017). Furthermore, deep ReLU networks often prefer learning simple functions (Valle-Perez et al., 2019; De Palma et al., 2019), specifically low-frequency functions (Rahaman et al., 2019), which are more robust to random parameter perturbations. Along this direction, here, we have shown that R networks (1) have smoother weights (Sec. 3.3.1), (2) prefer even simpler and fewer inputs (Sec. 3.3.2) than standard deep networks—i.e. R networks represent even simpler functions. Such simplicity biases are consistent with the fact that gradient images of R networks are much smoother (Tsipras et al., 2019) and that R classifiers act as a strong image prior for image synthesis (Santurkar et al., 2019).

**Robustness** Each R neuron computing a more restricted function than an S neuron (Sec. 3.3.2) implies that R models would require more neurons to mimic a complex S network. This is consistent with recent findings that adversarial training requires a larger model capacity (Xie and Yuille, 2020). In Sec. 3.3.1, we found that adversarial training produces network that are robust to images with additive Gaussian noise. Interestingly, Ford et al. (2019) found the reverse is also true: Training CNNs with additive Gaussian noise can improve the performance on adversarial examples.

While AdvProp did not yet show benefits on ResNet (Xie et al., 2020), it might be interesting future work to find out whether EfficientNets trained via AdvProp also have shape and simplicity biases. Furthermore, simplicity biases may be incorporated as regularizers into future training algorithms to improve model robustness. For example, encouraging filters to be smoother might improve robustness to high-frequency noise. Also aligned with our findings, Rozsa and Boulton (2019) found that explicitly narrowing down the non-zero input regions of ReLUs can improve adversarial robustness.

## 5 Discussion and Conclusion

We found that R networks heavily rely on shape cues in contrast to S networks. One may fuse an S network and a R network (two channels, one uses texture and one uses shape) into a single, more robust, interpretable

ML model. That is, such model may (1) have better generalization on OOD data than S or R network alone and (2) enable an explanation to users on what features a network uses to label a given image.

Our study on how individual hidden neurons contribute to the R network shape preference (Sec. 3.4) revealed that texture-detector units are equally important to the texture-based and shape-based recognition. This is in contrast to a common hypothesis that texture detectors should be exclusively only useful to texture-biased recognition. Our surprising finding suggests that the categories of stimuli in the well-known Network Dissection (Bau et al., 2017) need to be re-labeled and also extended with low-frequency patterns e.g. single lines or silhouettes in order to more accurately quantify hidden representations.

It might be interesting future work to improve model performance by (1) training them jointly on adversarial examples and texture-less images; and (2) adding smoothness prior to network gradients and filters. Also, adding a smoothness prior to the gradient images or filters of convolutional networks may improve their generalization capability.

In sum, our work has revealed several intriguing properties of adversarially-trained networks, providing insights for future designs of classifiers robust to out-of-distribution examples.

## Acknowledgement

AN is supported by the National Science Foundation under Grant No. 1850117, NaphCare Foundation, and GPU donations from Nvidia.

## References

- Arpit D, Jastrzebski S, Ballas N, Krueger D, Bengio E, Kanwal MS, Maharaj T, Fischer A, Courville A, Bengio Y, et al. (2017) A closer look at memorization in deep networks. In: Proceedings of the 34th International Conference on Machine Learning-Volume 70, JMLR. org, pp 233–242
- Bansal N, Agarwal C, Nguyen A (2020) Sam: The sensitivity of attribution methods to hyperparameters. In: Proceedings of the IEEE conference on computer vision and pattern recognition
- Bau D, Zhou B, Khosla A, Oliva A, Torralba A (2017) Network dissection: Quantifying interpretability of deep visual representations. In: Proceedings of the IEEE conference on computer vision and pattern recognition, pp 6541–6549
- Brendel W, Bethge M (2019) Approximating CNNs with bag-of-local-features models works surprisingly well on imagenet. In: International Conference on Learning Representations
- Caesar H, Uijlings J, Ferrari V (2018) Coco-stuff: Thing and stuff classes in context. In: Proceedings of the IEEE Conference on Computer Vision and Pattern Recognition, pp 1209–1218
- Chen LC, Papandreou G, Kokkinos I, Murphy K, Yuille AL (2017) Deeplab: Semantic image segmentation with deep convolutional nets, atrous convolution, and fully connected crfs. *IEEE transactions on pattern analysis and machine intelligence* 40(4):834–848
- De Palma G, Kiani B, Lloyd S (2019) Random deep neural networks are biased towards simple functions. In: *Advances in Neural Information Processing Systems*, pp 1962–1974
- Engstrom L, Ilyas A, Santurkar S, Tsipras D (2019) Robustness (python library). URL <https://github.com/MadryLab/robustness>
- Engstrom L, Ilyas A, Santurkar S, Tsipras D, Tran B, Madry A (2020) Adversarial robustness as a prior for learned representations. URL <https://openreview.net/forum?id=rygvFyrKwH>
- Ford N, Gilmer J, Cubuk ED (2019) Adversarial examples are a natural consequence of test error in noise. URL <https://openreview.net/forum?id=S1xoy3CcYX>
- Gatys LA, Ecker AS, Bethge M (2016) Image style transfer using convolutional neural networks. In: Proceedings of the IEEE conference on computer vision and pattern recognition, pp 2414–2423
- Geirhos R, Temme CR, Rauber J, Schütt HH, Bethge M, Wichmann FA (2018) Generalisation in humans and deep neural networks. In: *Advances in Neural Information Processing Systems*, pp 7538–7550
- Geirhos R, Rubisch P, Michaelis C, Bethge M, Wichmann FA, Brendel W (2019) Imagenet-trained CNNs are biased towards texture; increasing shape bias improves accuracy and robustness. In: International Conference on Learning Representations, URL <https://openreview.net/forum?id=Bygh9j09KX>
- Gilmer J, Ford N, Carlini N, Cubuk E (2019) Adversarial examples are a natural consequence of test error in noise. In: International Conference on Machine Learning, pp 2280–2289
- Goyal A, Bengio Y (2020) Inductive biases for deep learning of higher-level cognition. arXiv preprint arXiv:201115091
- He K, Zhang X, Ren S, Sun J (2016) Deep residual learning for image recognition. In: Proceedings of the IEEE conference on computer vision and pattern recognition, pp 770–778
- Hendrycks D, Dietterich T (2019) Benchmarking neural network robustness to common corruptions and perturbations. In: International Conference on Learning Representations, URL <https://openreview.net/forum?id=HJz6tiCqYm>
- ImageMagick (2020) Imagemagick. URL <https://imagemagick.org>
- Krizhevsky A, Sutskever I, Hinton GE (2012) Imagenet classification with deep convolutional neural networks. In: *Advances in neural information processing systems*, pp 1097–1105
- Madry A, Makelov A, Schmidt L, Tsipras D, Vladu A (2018) Towards deep learning models resistant to adversarial attacks. In: International Conference on Learning Representations, URL <https://openreview.net/forum?id=rJzIBfZAb>
- Nguyen A, Yosinski J, Clune J (2015) Deep neural networks are easily fooled: High confidence predictions for unrecognizable images. In: *Computer Vision and Pattern Recognition (CVPR)*
- Nguyen A, Dosovitskiy A, Yosinski J, Brox T, Clune J (2016a) Synthesizing the preferred inputs for neurons in neural networks via deep generator networks. In: *Advances in neural information processing systems*, pp 3387–3395
- Nguyen A, Yosinski J, Clune J (2016b) Multifaceted feature visualization: Uncovering the different types of features learned by each neuron in deep neural networks. In: *Visualization for Deep Learning Workshop, ICML conference*
- Nguyen A, Yosinski J, Clune J (2019) Understanding neural networks via feature visualization: A survey. In: *Explainable AI: Interpreting, Explaining and Visualizing Deep Learning*, Springer, pp 55–76
- PyTorch (2019) torchvision.models — pytorch master documentation. <https://pytorch.org/docs/s>

- [table/torchvision/models.html](#), (Accessed on 09/21/2019)
- Rahaman N, Baratin A, Arpit D, Dräxler F, Lin M, Hamprecht FA, Bengio Y, Courville AC (2019) On the spectral bias of neural networks. In: ICML, pp 5301–5310
- Rozsa A, Boulton TE (2019) Improved adversarial robustness by reducing open space risk via tent activations. arXiv preprint arXiv:1908.02435
- Rudin LI, Osher S, Fatemi E (1992) Nonlinear total variation based noise removal algorithms. *Physica D: nonlinear phenomena* 60(1-4):259–268
- Russakovsky O, Deng J, Su H, Krause J, Satheesh S, Ma S, Huang Z, Karpathy A, Khosla A, Bernstein M, et al. (2015) Imagenet large scale visual recognition challenge. *International journal of computer vision* 115(3):211–252
- Salman H, Ilyas A, Engstrom L, Kapoor A, Madry A (2020) Do adversarially robust imagenet models transfer better? *Advances in Neural Information Processing Systems* 33
- Santurkar S, Ilyas A, Tsipras D, Engstrom L, Tran B, Madry A (2019) Image synthesis with a single (robust) classifier. In: Wallach H, Larochelle H, Beygelzimer A, d'Alché-Buc F, Fox E, Garnett R (eds) *Advances in Neural Information Processing Systems*, Curran Associates, Inc., vol 32, pp 1262–1273, URL <https://proceedings.neurips.cc/paper/2019/file/6f2268bd1d3d3ebaabb04d6b5d099425-Paper.pdf>
- Szegedy C, Zaremba W, Sutskever I, Bruna J, Erhan D, Goodfellow I, Fergus R (2014) Intriguing properties of neural networks. In: *International Conference on Learning Representations*, URL <http://arxiv.org/abs/1312.6199>
- Szegedy C, Liu W, Jia Y, Sermanet P, Reed S, Anguelov D, Erhan D, Vanhoucke V, Rabinovich A (2015) Going deeper with convolutions. In: *Proceedings of the IEEE conference on computer vision and pattern recognition*, pp 1–9
- Tsipras D, Santurkar S, Engstrom L, Turner A, Madry A (2019) Robustness may be at odds with accuracy. In: *International Conference on Learning Representations*, URL <https://openreview.net/forum?id=SyxAb30cY7>
- Valle-Perez G, Camargo CQ, Louis AA (2019) Deep learning generalizes because the parameter-function map is biased towards simple functions. In: *International Conference on Learning Representations*, URL <https://openreview.net/forum?id=rye4g3AqFm>
- Xie C, Yuille A (2020) Intriguing properties of adversarial training at scale. In: *International Conference on Learning Representations*, URL [view.net/forum?id=HyxJhCEFDs](https://openreview.net/forum?id=HyxJhCEFDs)
- Xie C, Tan M, Gong B, Wang J, Yuille AL, Le QV (2020) Adversarial examples improve image recognition. In: *Proceedings of the IEEE/CVF Conference on Computer Vision and Pattern Recognition*, pp 819–828
- Yin D, Gontijo Lopes R, Shlens J, Cubuk ED, Gilmer J (2019) A fourier perspective on model robustness in computer vision. *Advances in Neural Information Processing Systems* 32:13276–13286
- Yosinski J, Clune J, Bengio Y, Lipson H (2014) How transferable are features in deep neural networks? In: *Advances in Neural Information Processing Systems*, pp 3320–3328
- Zhang T, Zhu Z (2019) Interpreting adversarially trained convolutional neural networks. In: *International Conference in Machine Learning*

## A Convolutional layers used in Network Dissection analysis

For both standard and robust models, we ran NetDissect on 5 convolutional layers in AlexNet (Krizhevsky et al., 2012), 12 in GoogLeNet (Szegedy et al., 2015), and 5 in ResNet-50 architectures (He et al., 2016). For each layer, we use after-ReLU activations (if ReLU exists).

*AlexNet* layers: conv1, conv2, conv3, conv4, conv5. Refer to these names in Krizhevsky et al. (2012).

*GoogLeNet* layers: conv1, conv2, conv3, inception3a, inception3b, inception4a, inception4b, inception4c, inception4d, inception4e, inception5a, inception5b

Refer to these names in PyTorch code <https://github.com/pytorch/vision/blob/master/torchvision/models/googlenet.py#L83-L101>.

*ResNet-50* layers: conv1, layer1, layer2, layer3, layer4

Refer to these names in PyTorch code <https://github.com/pytorch/vision/blob/master/torchvision/models/resnet.py#L145-L155>.

## B Kernel smoothness visualization

We visualize the conv1 weights of the 6 models and plot them side by side to compare their kernel smoothness (Fig. A1). The kernels in R models are consistently smoother than its counterpart. For a more straightforward visualization, we use Spearman rank correlation score to pair the similar kernels in AlexNet and AlexNet-R (Fig. A2).

## C Object and color detectors of AlexNet

We compared the layer-wise difference of object and color detectors of AlexNet and AlexNet-R (Fig. A3). We can see in Fig. A3a that AlexNet has more object detectors and fewer color detectors compared to AlexNet-R.

## D Total variance (TV) of AlexNet & AlexNet-R on clean/noisy images

The total variances of AlexNet & AlexNet-R plot (Fig. A4) shows that the early layer i.e. conv1 in AlexNet-R can filter out Gaussian noise. The total variances of clean and noisy input results in similar value in conv1 in AlexNet-R, this means the noise has been filtered by conv1.

## E ImageNet-C evaluation

In Table A1, we evaluate the validation accuracy of 6 models on 15 common types of image corruptions in ImageNet-C. It turns out that shape biased model does not necessarily mean better generalization on these image corruptions.



Fig. A1: All 64 conv1 filters of in each standard network (left) and its counterpart (right). The filters of R models (right) are smoother and less diverse compared to those in standard models (left). Especially, the edge filters of standard networks are noisier and often contain multiple colors in them.

## F Examples of shape-less and texture-less images

We randomly choose one image in 7 COCO coarser classes (out of 16) and plot the corresponding shape-less and texture-less version (Fig. A5).

## G Visualizing channel preference via cue-conflict and NetDissect

In Fig. A6- A8, **Top** is the top-49 images of the channels (Similar to Fig. 7). On the **Middle & Bottom**, we zero-out

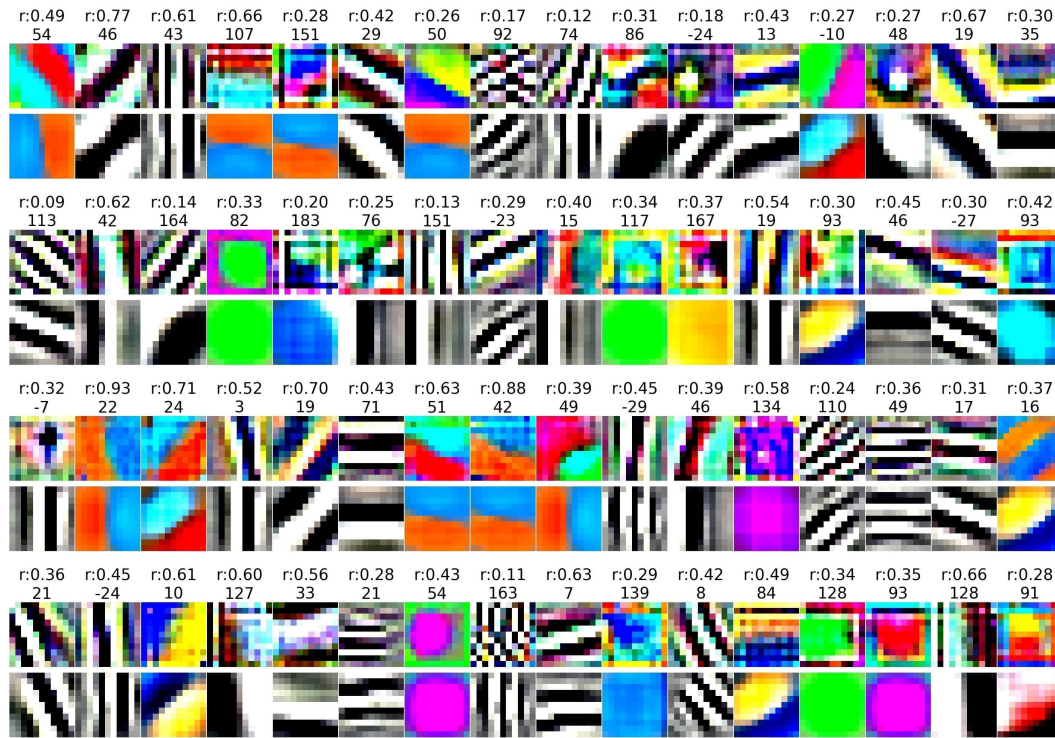
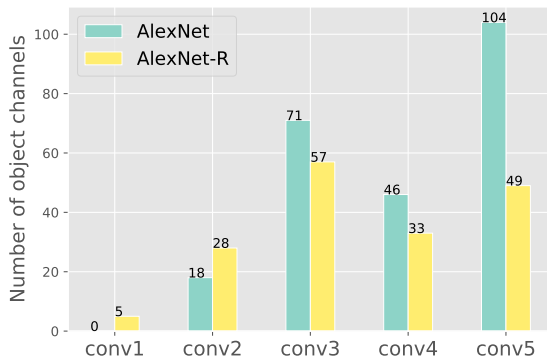


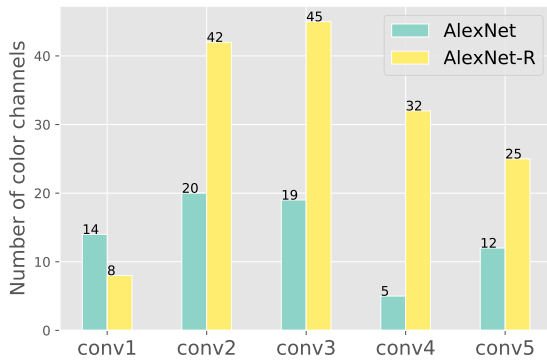
Fig. A2: conv1 filters of AlexNet-R are smoother than the filters in standard AlexNet. In each column, we show an AlexNet filter conv1 filter and their nearest filter (bottom) from the AlexNet-R. Above each pair of filters are their Spearman rank correlation score (e.g.  $r: 0.36$ ) and their total variation (TV) difference (i.e. smoothness differences). Standard AlexNet filters are mostly noisier than their nearest R filter (i.e. positive TV differences).

Table A1: Top-1 accuracy of 6 models (in %) on all 15 types of image corruptions in ImageNet-C (Hendrycks and Dietterich, 2019). On average over all 15 distortion types, R models underperform their standard counterparts.

		AlexNet	AlexNet-R	GoogLeNet	GoogLeNet-R	ResNet	ResNet-R
(a) Noise	Gaussian	10.79	<b>55.95</b>	<b>56.36</b>	26.56	<b>45.72</b>	33.57
	Shot	10.93	<b>53.12</b>	<b>50.39</b>	24.53	41.42	<b>43.61</b>
	Impulse	8.66	<b>52.15</b>	<b>42.23</b>	24.70	<b>45.45</b>	41.18
(b) Blur	Defocus	23.93	<b>27.51</b>	<b>39.11</b>	26.00	<b>52.42</b>	37.40
	Glass	22.47	<b>42.90</b>	22.41	<b>42.78</b>	24.92	<b>50.93</b>
	Motion	33.37	<b>41.05</b>	<b>43.57</b>	40.669	<b>52.78</b>	49.43
	Zoom	38.55	<b>44.02</b>	42.33	<b>43.30</b>	<b>52.43</b>	51.75
(c) Weather	Snow	26.08	26.32	<b>53.09</b>	15.40	<b>48.92</b>	39.89
	Frost	<b>21.42</b>	13.47	<b>46.48</b>	8.31	<b>44.08</b>	32.99
	Fog	<b>27.71</b>	1.59	<b>65.16</b>	12.00	<b>64.46</b>	3.72
	Brightness	<b>77.65</b>	62.48	<b>92.20</b>	51.55	<b>90.99</b>	79.99
(d) Digital	Contrast	<b>18.07</b>	1.94	<b>79.00</b>	22.34	<b>61.50</b>	3.40
	Elastic	76.00	<b>82.49</b>	78.32	78.37	74.85	<b>82.72</b>
	Pixelate	57.70	<b>80.68</b>	<b>82.66</b>	80.96	71.14	<b>83.83</b>
	JPEG	72.65	<b>87.50</b>	80.73	<b>83.93</b>	82.71	<b>86.60</b>
(e) Extra	Speckle Noise	15.46	<b>25.71</b>	<b>36.34</b>	23.96	<b>35.66</b>	31.03
	Gaussian Blur	21.29	22.18	<b>32.58</b>	23.76	26.78	<b>29.27</b>
	Spatter	<b>28.25</b>	25.89	<b>44.23</b>	36.37	<b>50.11</b>	40.96
	Saturate	<b>34.17</b>	22.23	<b>61.31</b>	35.55	<b>62.37</b>	42.55
<b>mean Accuracy</b>		35.06	<b>44.94</b>	<b>58.27</b>	38.76	<b>56.92</b>	48.80



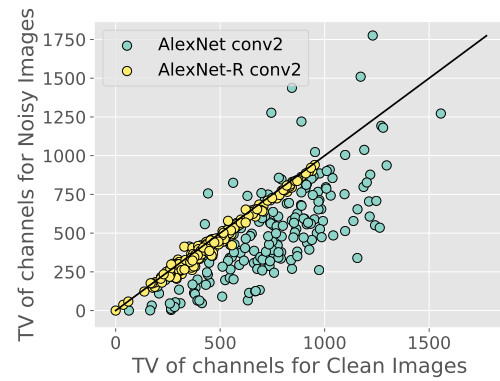
(a) Number of object detectors per AlexNet layer



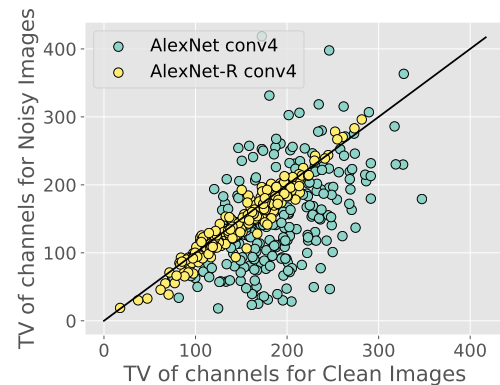
(b) Number of color detectors per AlexNet layer

Fig. A3: In higher layers (here, conv4 and conv5), AlexNet-R have fewer object detectors but more color detector units compared to standard AlexNet. The differences between the two networks increase as we go from lower to higher layers. Because both networks share an identical architecture, the plots here demonstrate a substantial shift in the functionality of the neurons as the result of adversarial training—detecting more colors and textures and fewer objects. Similar trends were also observed between standard and R models of GoogLeNet and ResNet-50 architectures.

the corresponding channel and re-run the conflict test to find out the images that were mis-classified. i.e. Fig.A6 the clock images in **Middle** were classified into shape category by cue-conflict test. After zeroing-out the channel, the network lose the ability to classify the image into shape category.



(a) conv2



(b) conv4

Fig. A4: Each point shows the Total Variation (TV) of the activation maps on clean and noisy images for an AlexNet or AlexNet-R channel. We observe a striking difference in conv1: The smoothness of R channels remains unchanged before and after noise addition, explaining their superior performance in classifying noisy images. While the channel smoothness differences (between two networks) are gradually smaller in higher layers, we still observe R channels are consistently smoother.

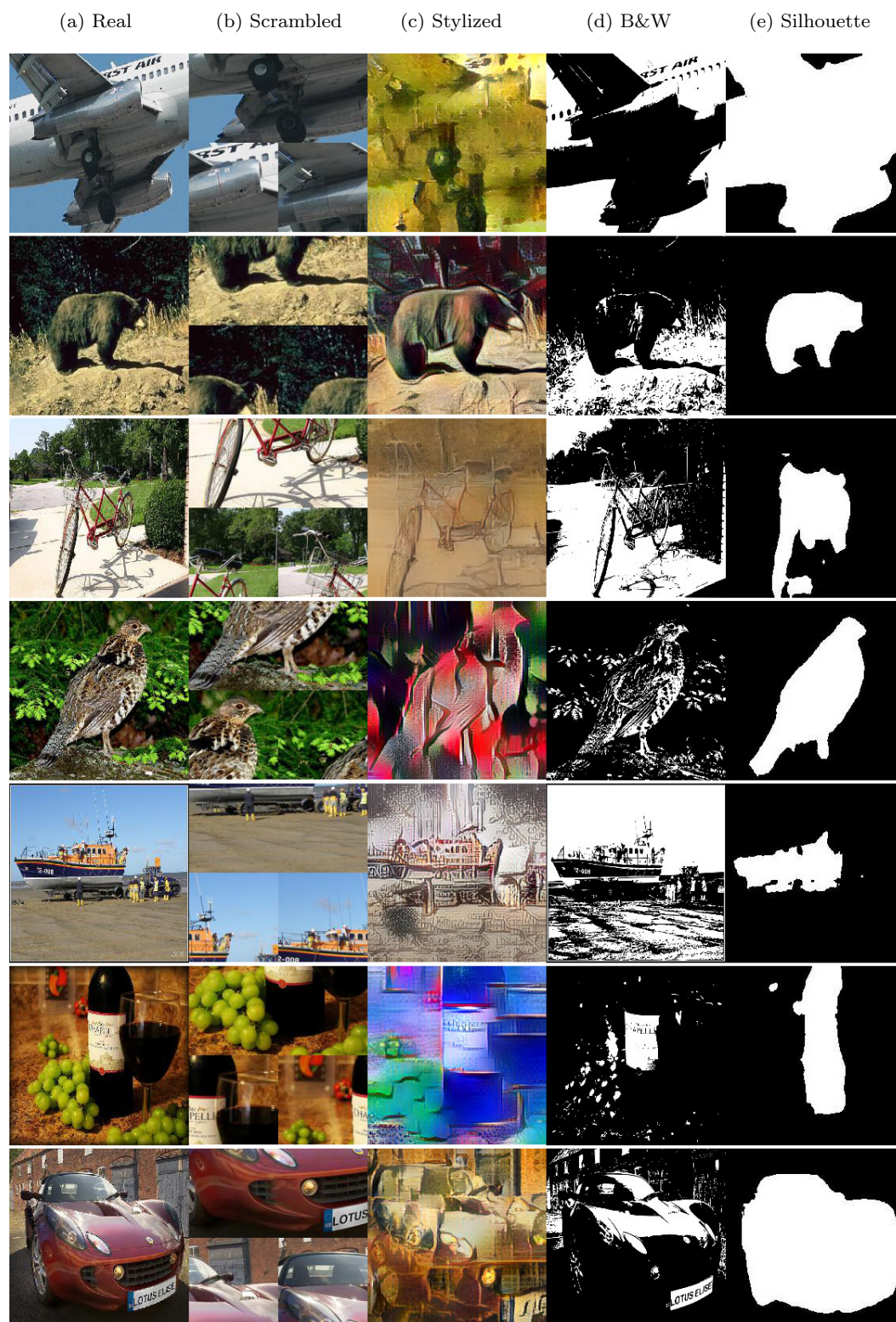


Fig. A5: Applying different transformation that remove shape/texture on real images. We randomly show an example of 7 out of 16 COCO coarser classes. See Table 3 for classification accuracy scores on different images distortion dataset in 1000 classes(Except for Silhouette). *\*Note: Silhouette are validate in 16 COCO coarse classes.*

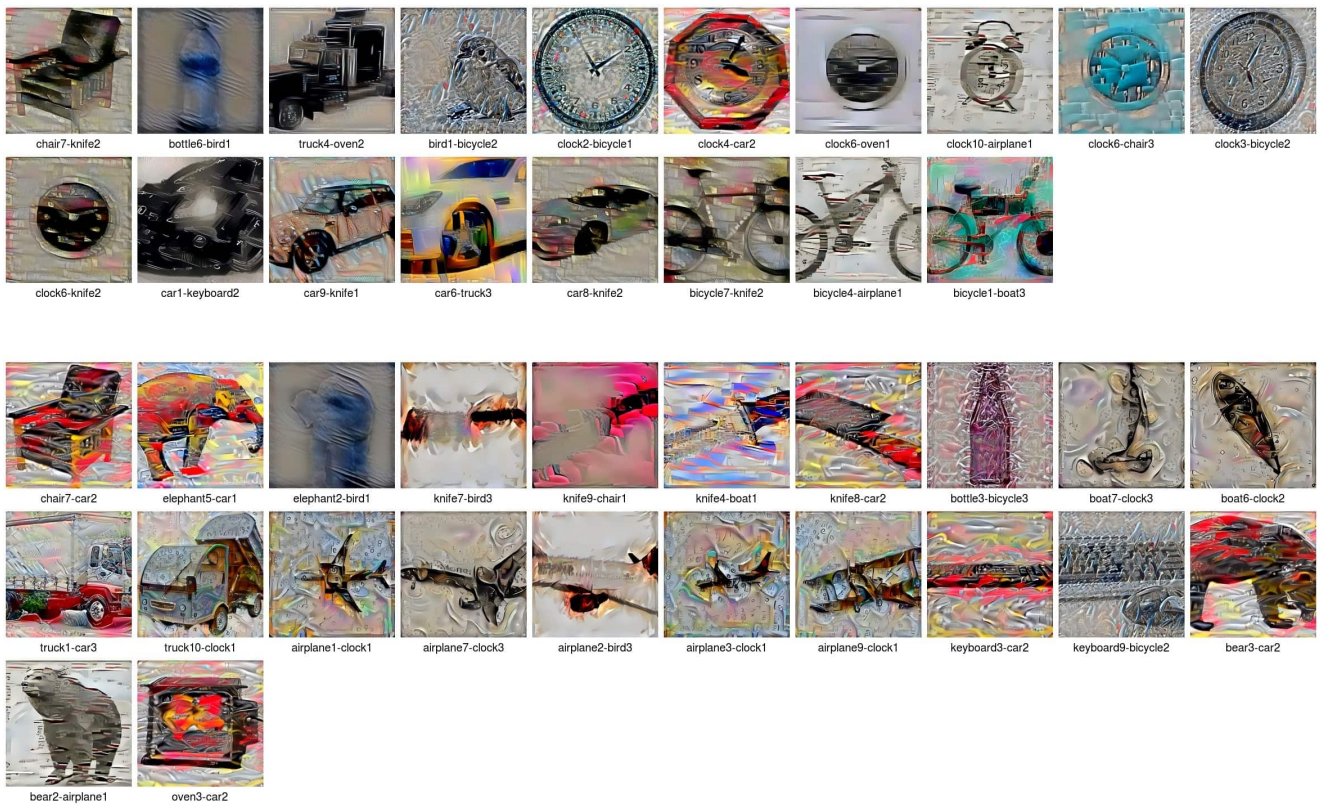
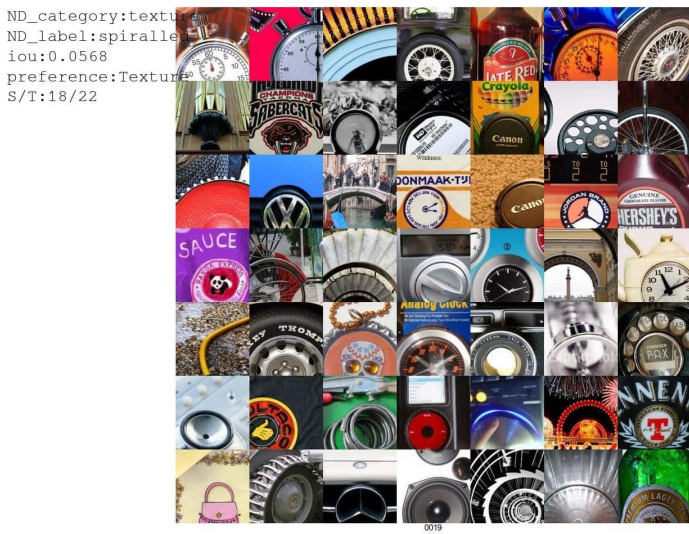


Fig. A6: AlexNet conv<sub>4</sub><sub>19</sub> with Shape and Texture scores of 18 and 22, respectively. It has a NetDissect label of spiralled (IoU: 0.0568) under texture category. Although this neuron is in NetDissect texture category, the misclassified images suggest that this neuron helps in both shape- and texture-based recognition. **Top:** Top-49 images that highest-activated this channel. **Middle:** Mis-classified images in shape category (18 images). **Bottom:** Mis-classified images in texture category (22 images).

```

ND_category:text
ND_label:banded
iou:0.0409999999
preference:Textu
S/T:17/19
    
```

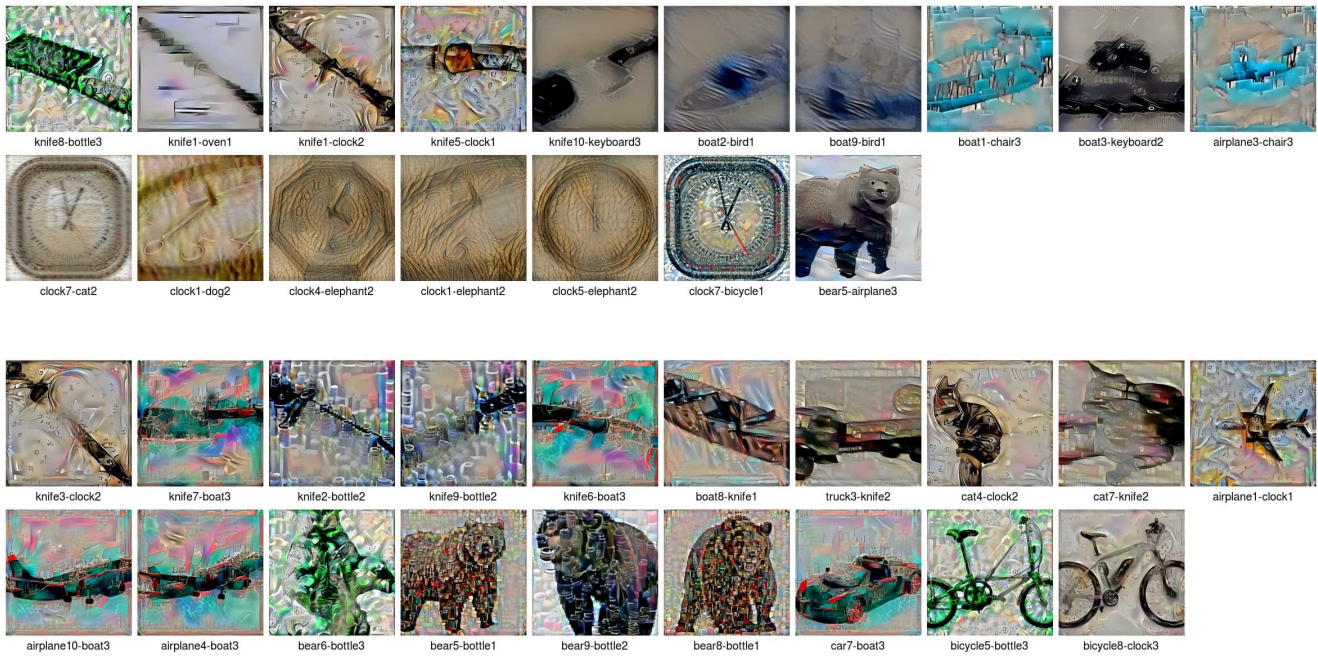
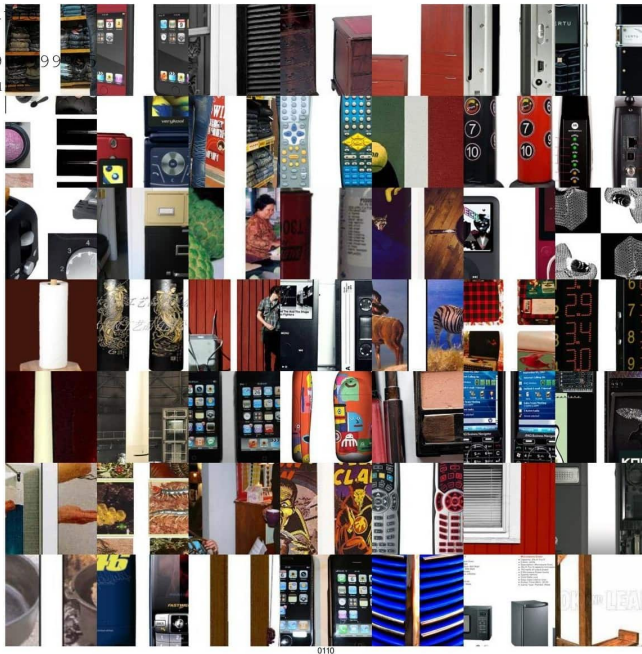


Fig. A7: AlexNet-R conv5<sub>110</sub> with Shape and Texture scores of 17 and 19, respectively. It has a NetDissect label of banded (IoU: 0.0409) under texture category. This neuron has almost equal Shape and Texture scores and is useful in detecting both the shape and textures of knives and bottles at the same time. **Top:** Top-49 images that highest-activated this channel. **Middle:** Mis-classified images in shape category. **Bottom:** Mis-classified images in texture category.

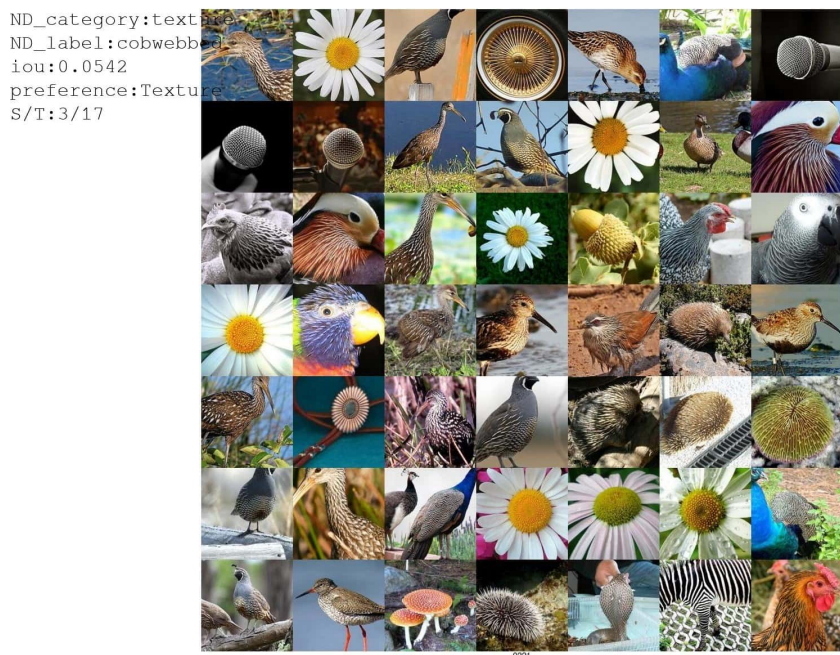
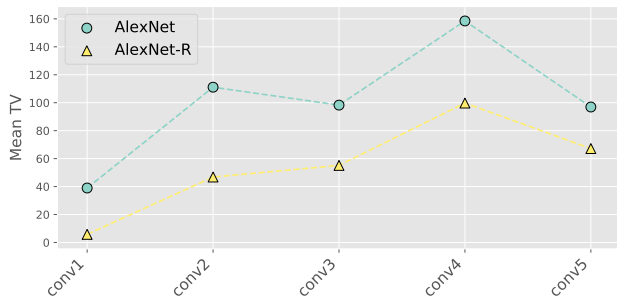
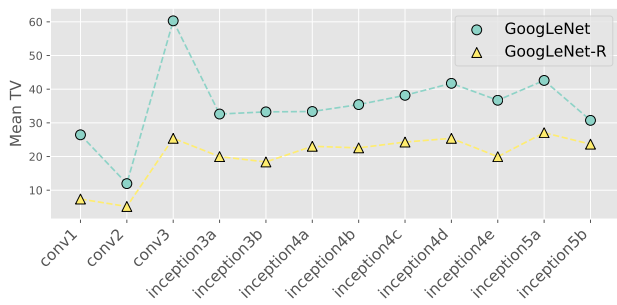


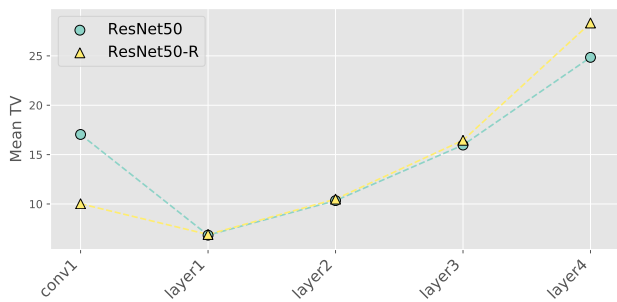
Fig. A8: AlexNet conv5<sub>221</sub> with Shape and Texture scores of 3 and 17, respectively. It has a NetDissect label of cobwebbed (IoU: 0.0542) under texture category. This is a heavily texture-biased neuron that helps networks detect animals by their fur textures. **Top:** Top-49 images that highest-activated this channel. **Middle:** Mis-classified images in shape category. **Bottom:** Mis-classified images in texture category.



(a) Mean layer-wise kernel TV of AlexNet and AlexNet-R

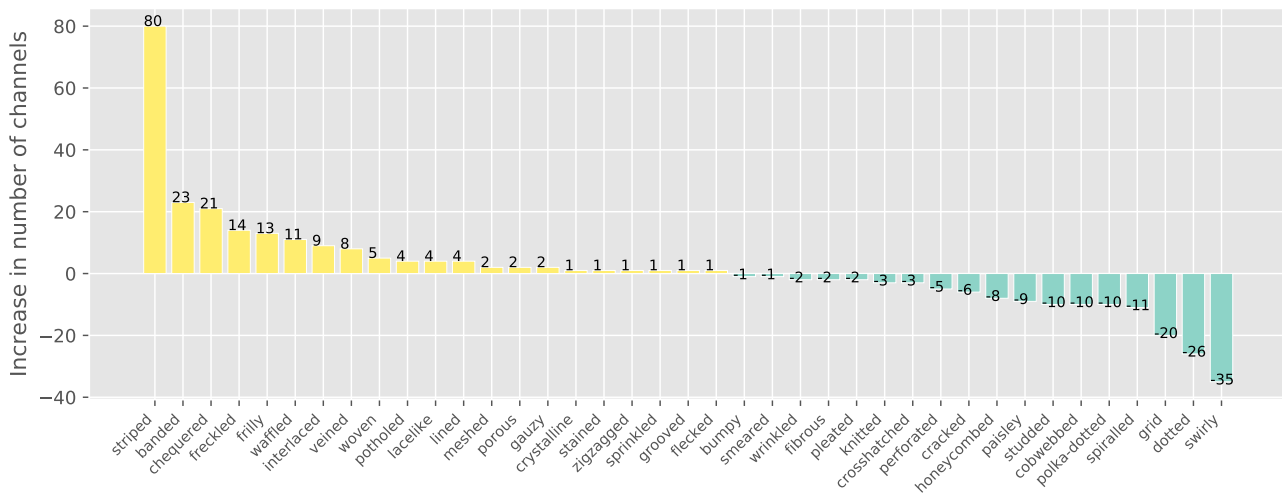


(b) Mean layer-wise kernel TV of GoogLeNet and GoogLeNet-R

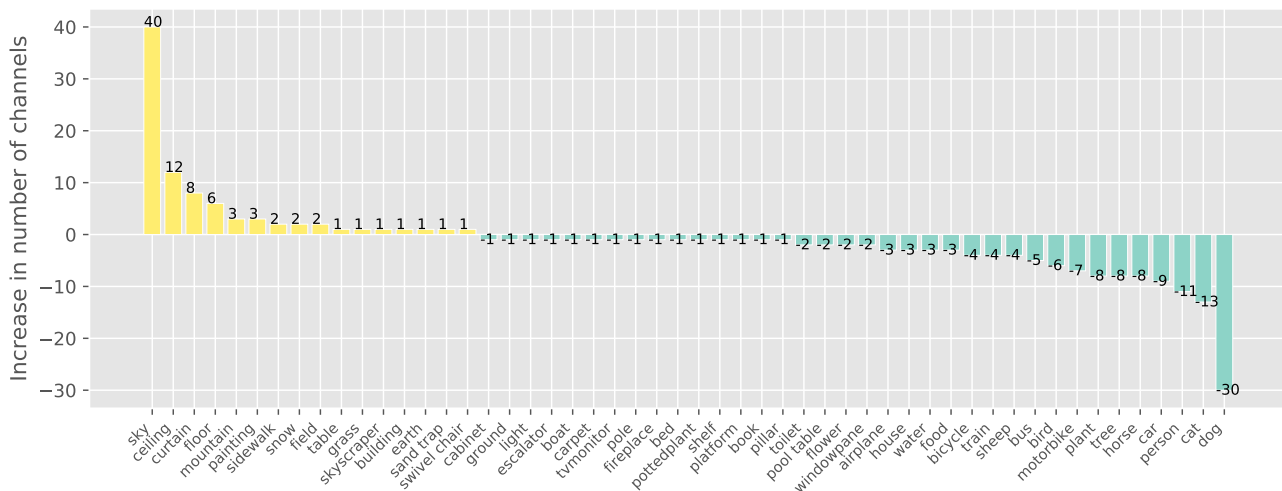


(c) Mean layer-wise kernel TV of ResNet and ResNet-R

Fig. A9: For all main conv layers, AlexNet-R filters are smoother (i.e. lower TV mean) than their counterparts in AlexNet (a). The same observation was found in GoogLeNet-R vs. GoogLeNet comparison (b). In ResNet-R, its early filters at conv1 are also smoother than those in ResNet.



(a) Differences in texture channels between AlexNet and AlexNet-R



(b) Differences in object channels between AlexNet and AlexNet-R

Fig. A10: In each bar plot, we column shows the difference in the number of channels (between AlexNet-R and AlexNet) for a given concept e.g. *striped* or *banded*. That is, yellow bars (i.e. positive numbers) show the count of channels that the R model has more than the standard network in the same concept. Vice versa, teal bars represent the concepts that R models have fewer channels. The NetDissect concept names are given in the x-axis.

**Top:** In the texture category, the R model has a lot more simple texture patterns e.g. *striped* and *banded* (see Fig. A11 for example patterns in these concepts).

**Bottom:** In the object category, AlexNet-R often prefers simpler-object detectors e.g. *sky* or *ceiling* (Fig. A10b; leftmost) while the standard network has more complex-objects detectors e.g. *dog* and *cat* (Fig. A10b; rightmost).

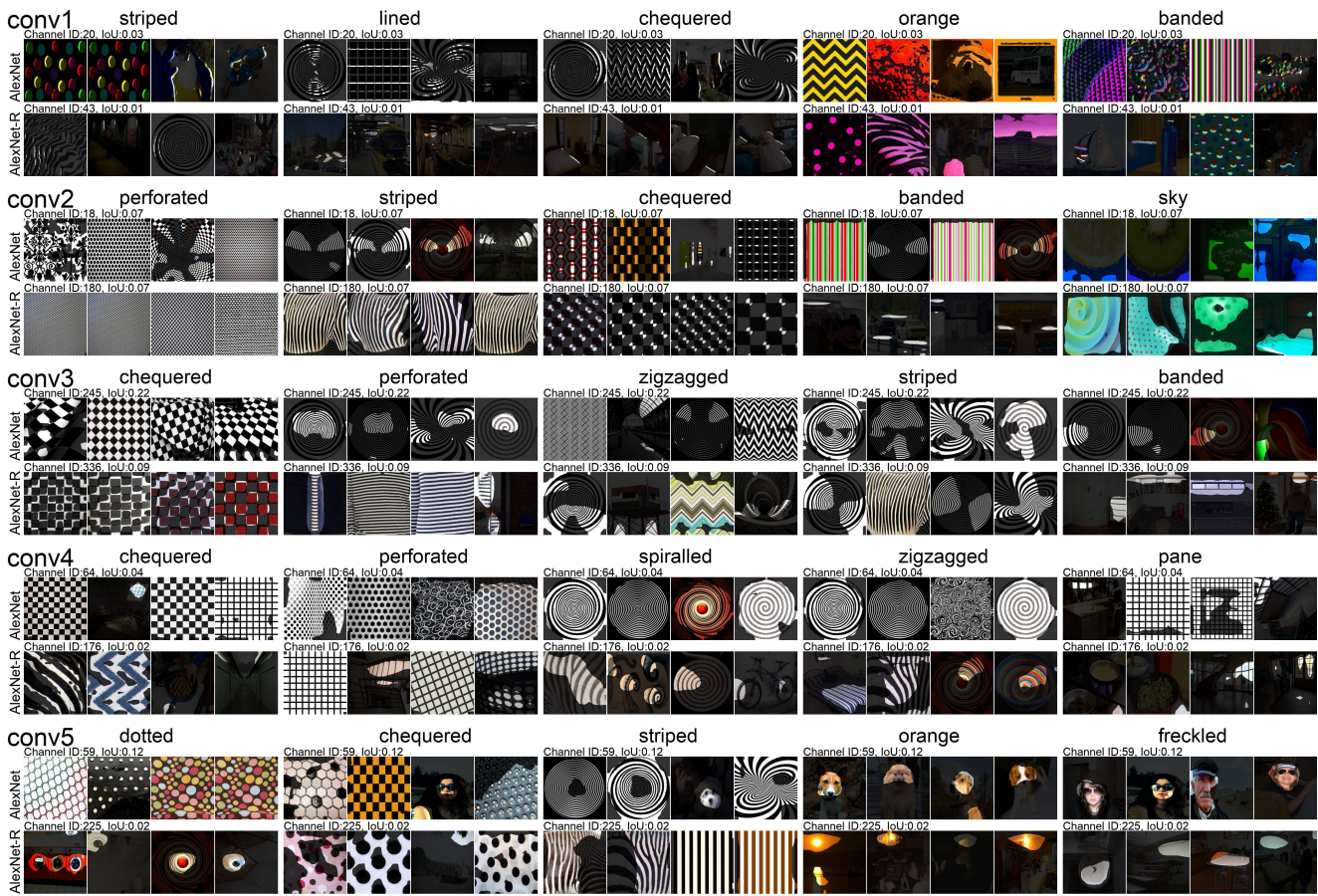


Fig. A11: The NetDissect images preferred by the channels in the top-5 most important concepts in AlexNet (i.e. highest accuracy drop when zeroed out; see Sec. 3.3.2). For each concept, we show the highest-IoU channels.

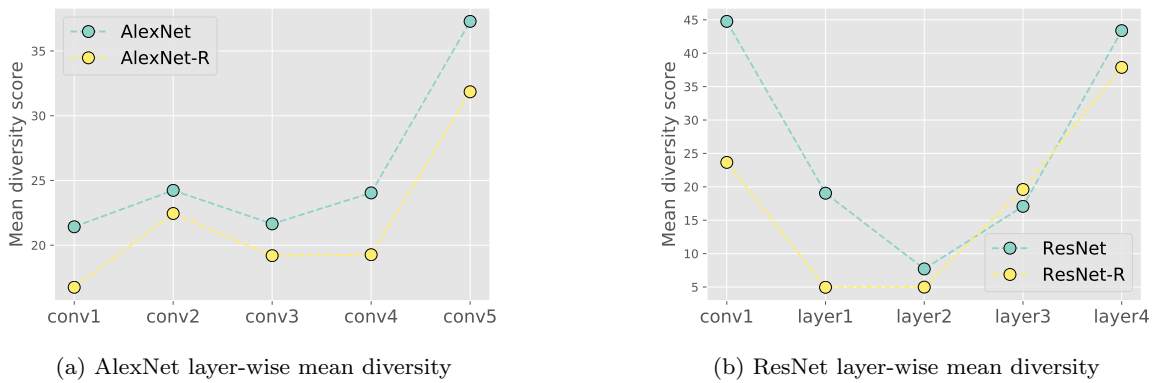


Fig. A12: In each plot, we show the mean diversity scores across all channels in each layer. Both AlexNet-R and ResNet-R consistently have channels with lower diversity scores (i.e. detecting fewer unique concepts) than the standard counterparts.